Available online at www.sciencedirect.com
SCIENCE DIRECT®
Journal of Power Sources 136 (2004) 376–382
JOURNAL OF POWER SOURCES
www.elsevier.com/locate/jpowsour

Development of ultra high power, valve-regulated lead-acid batteries for industrial applications

M. Luisa Soria*, Jesús Valenciano, Araceli Ojeda

Tudor-Exide Technologies, Global R&D Centre, Carretera N-II, km 42, E-19200 Azuqueca de Henares, Spain

Available online 9 June 2004

Abstract

There is a recent market trend towards industrial battery powered products that demand occasionally very high discharge rates. This fact is today solved by oversizing the battery or by using more expensive high power nickel-cadmium batteries. Within an EC funded project, ultra high power lead-acid batteries for UPS applications are being developed. The batteries are characterised by a thin electrode design linked to the use of novel separator materials to increase the battery life under floating and deep cycling conditions. Battery performance under different working conditions is presented, in comparison to standard products, and the battery improvements and failure mechanisms are also discussed.

Keywords: Valve-regulated-lead-acid batteries; High power batteries; Polyethylene membranes; Absorptive glass mats; UPS applications

1. Introduction

High power lead-acid batteries have traditionally been linked to automotive applications, mainly for vehicle starting, even at low temperatures [1,2]. However, novel industrial and automotive applications, such as 42 V and hybrid vehicles, demand an improved battery performance in terms of high power capability and cyclability. The use of advanced battery technologies, such as nickel/metal hydride or lithium-ion batteries, can provide such a performance, but cost is a quite restrictive factor for most of the industrial and automotive applications. This fact led to the definition in past years of a research project aimed at the development of ultra high power valve-regulated lead-acid (VRLA) batteries for uninterruptible power supply (UPS) applications, with increased power capability, life and reliability [3].

Nowadays UPS manufacturers demand batteries with very high specific power and relatively low specific energy, because most mains failures can be defined as “microfailures”, usually of the order of seconds and, moreover, some UPS users have a motor generator and the battery is only used during the motor starting. Due to these facts, it is not necessary to provide energy but power. Today, from smaller to bigger installations, VRLA batteries are the preferred choice, due to their intrinsic characteristics of lack of maintenance, ease of installation, even in the rack of the commuting equipment, no gas release, clean product, and cost [4].

Furthermore, future liberalisation of the electricity market and decentralised power generation, whether based on conventional or renewable energy sources, will demand the development of energy storage systems with high power capability and increased battery reliability and life for high quality electricity supply, peak load shaving and improved grid stability in a massive distributed or decentralised energy resources (DER) deployment situation.

Battery specific power is practically related to electrode area, so its increase, and therefore an electrode thickness reduction, appear essential to achieve the project objectives. Within this project, this has been achieved by means of the use of novel grid materials and grid manufacturing techniques, that allow an electrode thickness reduction to around 1 mm. Furthermore, it was necessary to achieve a similar size reduction in the conventional glass microfibre separator. But such thin material should have improved mechanical properties, for an adequate handling during the battery manufacturing processes, and could make the battery more prone to develop short circuits across the separator during the filling and formation (hydration shorts) or during the battery life.

In order to avoid this problem, a new microporous polyethylene membrane has been developed and tested, with excellent mechanical properties, high porosity and low pore size. For these reasons, the final separator configuration includes a combination of two materials, improved

* Corresponding author. Tel.: +34-949-263-316; fax: +34-949-262-560.
E-mail address: soriaml@tudor.es (M.L. Soria).

0378-7753/$ – see front matter © 2004 Elsevier B.V. All rights reserved.
doi:10.1016/j.jpowsour.2004.03.017

non-woven glass microfibre and the polyethylene membrane [5].

Moreover, the microporous membrane can provide an adequate barrier to oxygen generated during charge: as the saturation level in the separator decreases, the oxygen cycle draws an increasing amount of charging current, thus causing the negative plate depolarisation observed as failure mode in VRLA batteries during stand-by and cyclic use [6]. The membrane should slow down the transfer of oxygen to the negative plate, allowing a more complete recharge of the plate before oxygen recombination takes place.

2. Experimental

12 V prototype batteries have been assembled with commercial ABS containers sized 180 mm × 75 mm × 150 mm, which are commonly used in the manufacturing of 15 Ah gel VRLA batteries for stand-by applications. Positive and negative plates were prepared in a standard continuous manufacturing line, cured under standard conditions and then they were cut to size and stacked manually. A manual cast-on-strap (COS) tooling was used to weld the plate lugs and finally the ABS case and cover, and the valves were welded with a laboratory ultrasound device.

The optimised high density polyethylene membrane and the absorptive glass mat (AGM) were developed by Daramic Inc. and Bernard Dumas S.A., respectively, in a former stage of the project [5]. The characteristics of the materials used in the preparation of the batteries are included in Tables 1 and 2. As shown in Table 1, two samples of membrane were tested, prepared as sheets in laboratory scale and as rolls in a pilot installation, respectively. Both show similar physical and mechanical characteristics: relatively low electrical resistance due to the high porosity and low thickness values, together with a small average pore size and adequate mechanical strength for material handling during battery production. On the other hand, the newly developed glass microfibre separator BD 9055XP combined good mechanical strength and acid absorption, according to the specific surface area and capillarity rise values shown in Table 2, where the characteristics of the materials used in the AGM prototypes are also included.

Table 1
Properties of Daramic membrane samples

Sample	Lab sheets	Pilot rolls
Thickness (mm)	0.15	0.14
Electrical resistance (mΩ cm^2)	20	20
Porosity (%)	75.2	75.0
Average pore size (μm)	0.13	0.16
Elongation MD/CMD (%)	40/286	21/188
Tensile strength MD/CMD (N/mm^2)	14.0/2.6	15.8/3.1
Acid shrinkage MD (%)	+0.4	−1.0
Drying shrinkage MD (%)	−4.1	−3.3
Puncture strength (N)	6.8	4.8

MD: machine direction; CMD: cross machine direction.

Table 2
Bernard Dumas glassmat separator characteristics

	BD 6070XP	BD 9023XP	BD 9055XP
Basis weight (g/m^2)	115	38	100
Thickness (10 kPa, mm)	0.70	0.23	0.55
Density (g/m^2 for 1 mm thick, 10 kPa)	164.3	165.2	181.8
Porosity (% calculated, 10 kPa)	93	92.9	92.2
Specific surface area (BET, m^2/g)	0.90	1.46	1.49
Tensile strength MD/CMD (N/mm)	0.75/0.39	0.42/0.17	0.93/0.45
Elongation MD/CMD (%)	2.8/6.5	1.95/4.78	1.41/3.07
Puncture test (20 mm/min, g)	1200	280	520
Capillarity rise 2 min (mm)	65	60	58
Pore size (MFP, μm)	6.6	5.51	3.27

The nominal capacity of the batteries was defined as 18 Ah at the 8-h rate (C_8) and 15 Ah at the 1-h rate (C_1). Electrical testing was carried out with computer controlled cycling equipment: Bitrode LCN-7-100-12 and Digatron UBT BTS-550 ZLEG 300/150. High rate discharges were performed with a computer controlled Digatron UBT BTS-500 mod. HEW 2000-6BTS. Electrical testing included initial capacity check at different rates, power capability under constant power discharges, at rates ranging from 500 to 3000 W down to 9.0 V, determination of peak power and high rate charge acceptance at different states of charge and, finally, life under floating and deep cycle conditions. The floating test at 2.27 V/cell was accelerated at 55 °C. Capacity evolution at the C_8 and C_1 rates was checked every 42 days. According to Arrhenius law, each 42 day unit at 55 °C corresponds to 1.3 years of floating life at room temperature (20 °C). Cycle life was carried out according to IEC 896-2 specification, with 60% DoD discharges. Capacity evolution at the C_{10} rate was checked every 50 cycles. A tear-down analysis of the batteries was finally performed to establish the failure mode.

3. Results and discussion

Several parameters dealing with the active material composition and active material ratios have been studied to improve the battery performance in terms of power capability, life and reliability. The use of a combination of the polyethylene membrane and microfibre glassmat or only AGM materials as battery separator has also been considered in the different prototype groups.

Table 3
Characteristics and preliminary electrical testing of 12 V UHP VRLA prototypes (nominal capacity: 18 Ah)

	Standard AGM 12 V–15 Ah	UHP series			
		I	II	III	IV
Separator material	AGM	AGM	AGM	AGM + membrane (lab sheets)	AGM + membrane (pilot rolls)
Positive active material density (g/cm^3)	4.0	4.0	4.3	4.3	4.2
Battery weight (kg)	6.5	6.1	6.4	6.4	6.4
Internal resistance (mΩ, 1 kHz, 25 °C)	7.1	5.8	5.4	5.9	5.7
Capacity (Ah, 25 °C)					
C_{20} (0.9 A)	16.1	18.5	19.0	18.8	19.3
C_8 (2.25 A)	15.5	18.2	18.3	18.4	18.2
C_1 (15 A)	15.0	15.7	15.3	15.6	15.4

3.1. Prototype characteristics and initial capacity check

Table 3 summarises the characteristics and initial electrical performance of four groups of high power prototypes (UHP): the series I and II with only AGM separator layers and two different positive active material densities (4.0 and 4.3 g/cm^3) and the series III and IV with a combination of membrane + AGM layers, that correspond to prototypes with the membrane prepared at the laboratory and pilot installation scales, respectively. A group of conventional AGM batteries of the same size rated 15 Ah and designed for stand-by applications was also tested for comparison purposes. It is important to point out the great difference in the number of plates used in the standard AGM battery (three 3.5 mm positives and four 1.9 mm negatives) and in the UHP prototypes (eight 1.3 mm positives and seven 1.1 mm negatives).

Capacity values at the 20-h rate of UHP prototypes ranged from 18.5 to 19.3 Ah, versus 16.1 Ah for standard AGM batteries, and from 18.2 to 18.4 Ah versus 15.5 Ah at the 8-h discharge rate. UHP prototypes show therefore improved active material efficiency ratios and battery specific energy values due to the similar AGM battery and UHP prototype weight (6.5 kg versus 6.1–6.4 kg). The electrical resistance values mentioned in the table were measured with an AC Milliohmmeter after the preliminary testing and capacity check. Values obtained just after battery formation were around 0.5–1 mΩ higher.

3.2. Constant current discharges: Peukert curve

To establish the discharge performance at different rates, UHP prototypes series IV were discharged to 9.0 V under constant current conditions at the following rates: 0.9, 7.5, 15, 30, 75, 150 and 225 A. Fig. 1 shows the discharge current versus discharge duration in a logarithm scale, and also the linear regression of the values obtained (Peukert curve) that allows to estimate the battery performance under any other discharge conditions.

3.3. Constant power discharges

After the capacity check, the batteries were discharged down to 9.0 V at different constant power rates, from 500

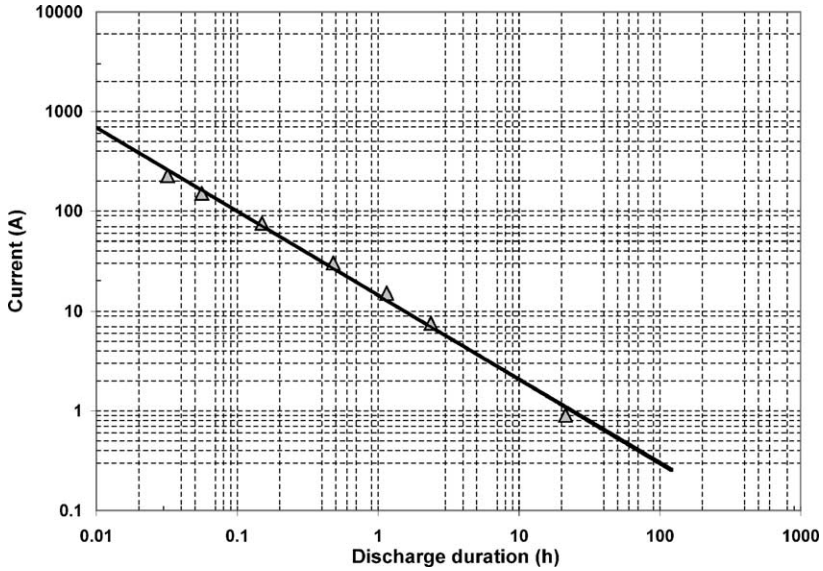

Fig. 1. Peukert curve of UHP prototypes series IV.

Table 4
Power capability of 12 V UHP VRLA prototypes

	Standard AGM	UHP series			
		I	II	III	IV
Constant power discharges (V_{min} > 9.0 V)					
500 W	10.4 min	17.4 min	17.0 min	17.0 min	17.0 min
650 W	6.9 min	11.9 min	12.3 min	12.4 min	12.2 min
1100 W	2.7 min	5.8 min	6.3 min	6.0 min	6.0 min
1500 W	1.1 min	3.45 min	3.8 min	3.4 min	3.55 min
2500 W	15 s	1.39 min	1.55 min	1.4 min	1.3 min
3000 W	–	55 s	56 s	50 s	47 s

to 3000 W, to establish their power capability in UPS and stand-by related applications. The discharge conditions and discharge durations are included in Table 4, and the results are represented in Fig. 2 as discharge power versus discharged energy.

Results show clearly that there is a huge difference between the standard AGM batteries and the UHP prototypes due to the thinner electrodes used in the latter prototype groups. However, the four groups of UHP prototypes show similar high rate capability performance, with small differences between the AGM and the membrane groups, correlated to the internal resistance values for the different groups of prototypes.

3.4. Peak power capability and high rate charge acceptance

High power capability and high rate charge acceptance are important battery features when future electricity network applications are aimed at, due to the market trend towards an increased integration of wind energy in the grid and the great concern about power quality in the future networks with a higher contribution of distributed energy generation. The 10 s peak power and 5 s high rate charge acceptance of UHP Prototypes series IV have been tested at different states of charge (SoC), ranging from 100 to 20%. Test results are shown in Fig. 3, represented as maximum charge and discharge power at the different states of charge considered. The peak power values were obtained at 400 A discharges and for the charge acceptance test, the maximum voltage was limited to 15 V (2.5 V/cell). A higher voltage value (i.e. 16 V or 2.65 V/cell) would lead to higher charge acceptance values, specially at low states of charge, however, it would be detrimental for battery life due to excessive gassing in case of prolonged high rate charging conditions (i.e. wind turbulences).

The best compromise between the peak power and charge acceptance values is obtained at a partial state of charge of around 60%: 3 kW in a 10 s discharge down to 10 V and 1350 W regenerative charge acceptance at 15 V.

3.5. Floating life

To estimate the life of the batteries according to standard floating conditions, the test was accelerated according to BS

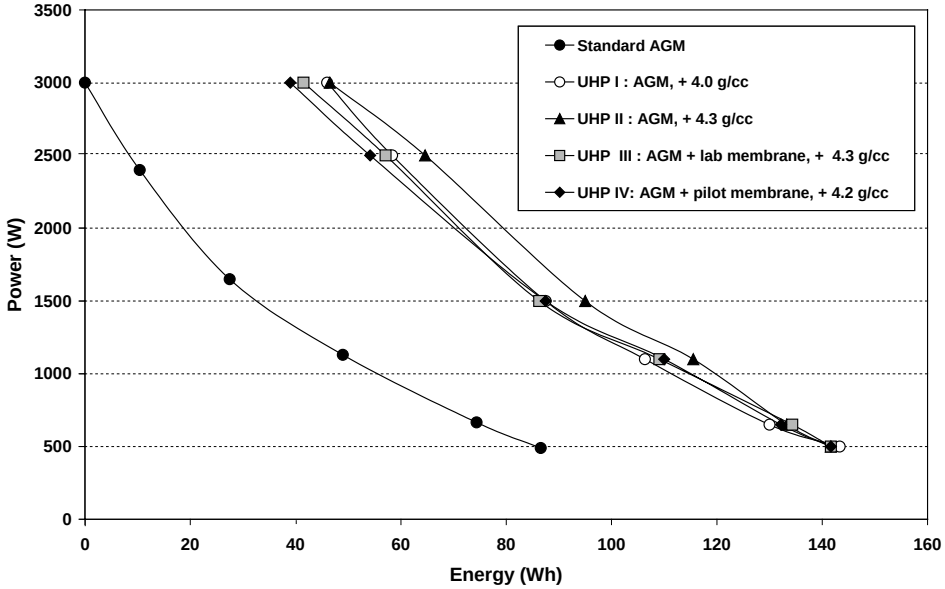

Fig. 2. Power vs. discharged energy of UHP prototypes and standard AGM batteries.

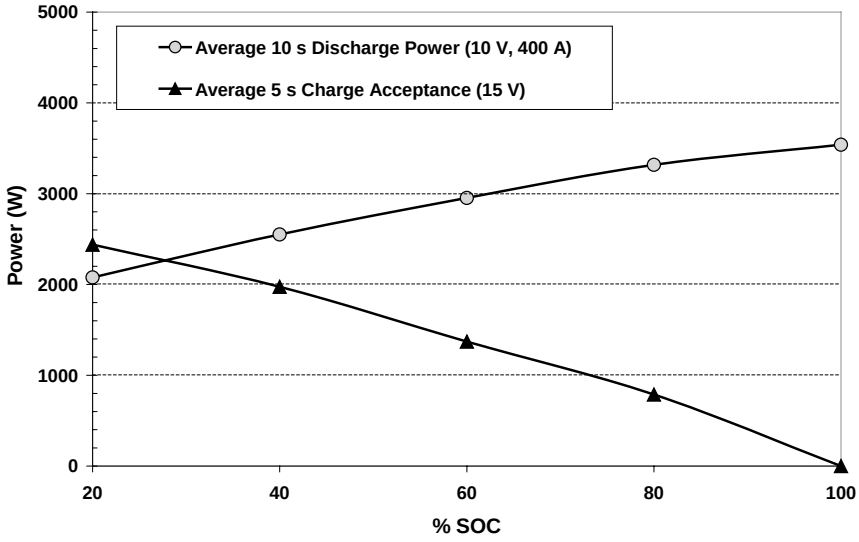

Fig. 3. Peak power and high rate charge acceptance of UHP prototypes.

6290 (1997) and performed overcharging at 2.27 V/cell and 55 °C. After each floating unit of 42 days, battery capacity at the 8- and 1-h rates was checked. Fig. 4 shows the capacity evolution at the 1-h rate of UHP prototypes series II (AGM) and IV (AGM + pilot membrane) compared to the AGM standard batteries. Before each capacity check, the prototypes were weighed and the internal resistance measured. The electrical resistance evolution of the three types of prototypes is also shown in the figure.

Results obtained show that, UHP prototypes have fulfilled over 200 days at 2.27 V/cell and 55 °C (between five and six 42-day units), equivalent to more than 6 years floating life at room temperature. On the other hand, standard AGM batteries have already fulfilled eight units at 2.27 V/cell and 55 °C (over 300 days), equivalent to nearly 10 years floating life at 20 °C, due to the thicker plate design: positive grids are three times thicker in standard AGM batteries than in UHP prototypes.

Corrosion of positive grids has been identified as the battery failure mode in all cases, and battery end of life is correlated with a high increase of the battery internal resistance, as shown in Fig. 4. In standard AGM batteries, with thick positive grids (3.5 mm), the capacity decays gradually, and a similar lineal trend is observed in the gradual increase of the battery internal resistance. However, UHP prototypes, with positive grids thinner than 1 mm, suffer a strong ca-

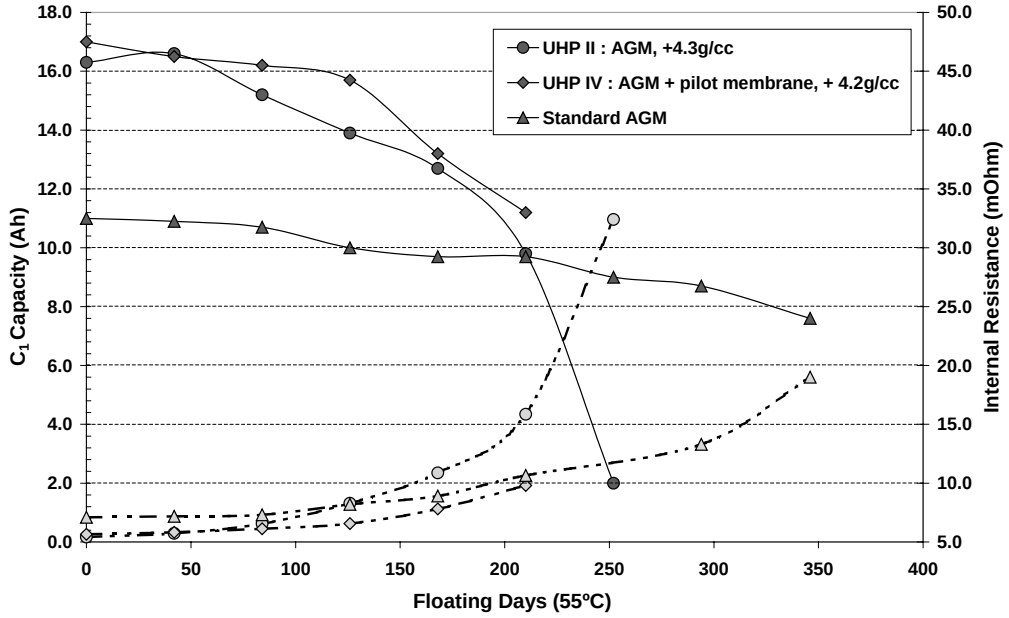

Fig. 4. One-hour rate capacity (▲) and electrical resistance (△) evolution of UHP prototypes and standard AGM batteries during accelerated floating test (2.27 V/cell and 55 °C).

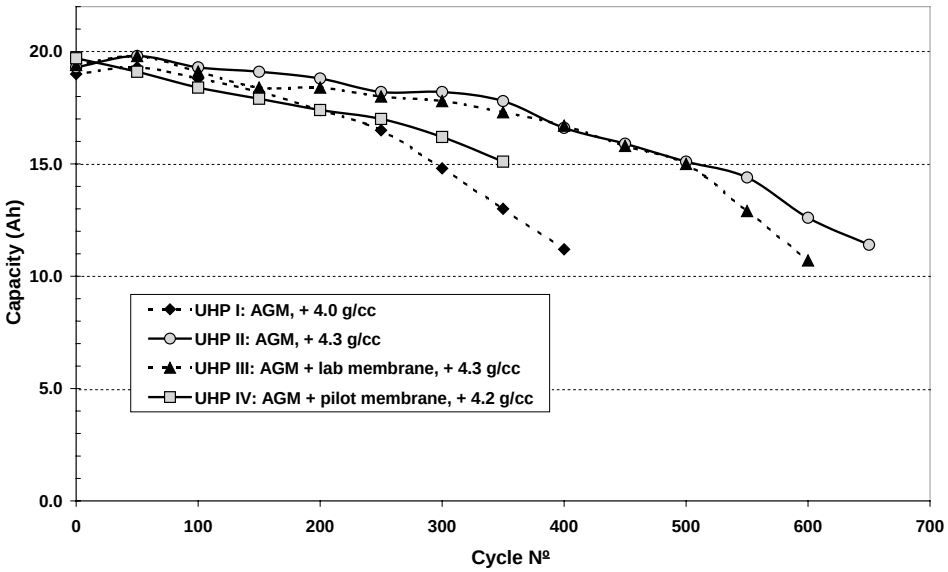

Fig. 5. Capacity evolution of UHP prototypes during cycle life test at 60% DoD.

pacity decay after 150–200 days of accelerated test, which is provoked by a sudden increase of the internal electrical resistance due to corrosion phenomena.

Weight loss records during the test have shown a significantly higher water loss in all the UHP prototype groups when compared to standard AGM batteries. This fact has been ascribed to the use of ABS containers in the prototypes, to ease the lab scale preparation conditions, whereas the standard AGM batteries use polypropylene containers, which show the advantage versus ABS containers of not being permeable to water.

3.6. Deep cycle life

Cycle life at 60% DoD has been tested according to IEC 896-2. The 10-h rate capacity evolution every 50 cycles of the four types of UHP prototypes is represented in Fig. 5. As shown in the figure, 400 cycles have been completed with the prototypes prepared with AGM separator and the lower positive paste density (4.0 g/cm^3), whereas the batteries with higher positive paste density (4.3 g/cm^3) have fulfilled around 600 cycles, for both the AGM and the membrane versions. Although the initial performance of the three types of UHP prototypes is similar, after 150 cycles the capacity decay slope is quite stronger in the prototypes with lower positive paste density.

Battery failure due to capacity decay has been ascribed to softening of the positive active material in all cases, as shown not only in the visual inspection of battery plates during the tear-down analysis but in the physico-chemical characterisation of materials as well. The chemical analysis of positive plates showed PbO_2 values around 95% in all cases, however, negative plates contained significant amounts of lead sulphate in the lower part of the plate: 20–45% depending on the number of cycles performed before battery failure, whereas in the upper part, sulphate content was <5%. This fact showed acid stratification in all types of UHP prototypes.

Table 5
Physical analysis of positive active material of UHP prototypes

Prototype reference	Paste density (g/cm^3)	Sample reference	Porosity (%)	Median pore diameter (μm)	Specific surface BET (m^2/g)
UHP I	4.0	Unformed plates	54.1	0.31	1.3
		Charged plates	52.3	0.70	5.1
		After 400 cycles	66.6	2.9	3.3
UHP II	4.3	Unformed plates	50.0	0.26	1.8
		Charged plates	N.A.	N.A.	N.A.
		After 650 cycles	65.1	3.6	3.1
UHP III	4.3	Unformed plates	50.0	0.26	1.8
		Charged plates	N.A.	N.A.	N.A.
		After 600 cycles	60.8	1.12	3.2
UHP IV	4.2	Unformed plates	51.3	0.32	1.6
		Charged plates	48.9	0.5	3.7
		After 400 cycles	61.2	2.2	3.1

Moreover, Table 5 shows the mercury intrusion porosimetry and the BET specific surface area results from positive active material of the different groups of batteries: during the battery formation, porosity decreases and pore size increases and later during cycling, there is a clear increase in the porosity and average pore size of the active material. This active material degradation is accelerated in the prototypes prepared with lower active material density (4.0 g/cm^3 versus 4.3 g/cm^3). On the other hand, BET specific surface increases during battery formation from around 1.5 to 4–5 m^2/g and then decreases during the life to around 3 m^2/g.

4. Conclusions

High power valve-regulated lead-acid batteries have been assembled using thin electrodes (around 1 mm thick) and a combination of improved glass mat (AGM) and thin polyethylene membrane as separator. Electrical testing showed excellent high power performance, even at the 30 s to 1 min discharge rates, linked to a relevant life under floating and deep cycle conditions. The 18 Ah batteries provided 10 s power peaks of 3.5 kW full of charge and 3 kW at 60% SoC. On the other hand, over 500 deep cycles (60% DoD) have been obtained and over 5 years floating life at room temperature can also be expected.

The development of high power lead-acid batteries with improved life and reliability can provide a cost effective solution for high power cyclic applications in which other battery types are used today (Ni/Cd, Ni/MH, etc.). In all these applications UHP VRLA batteries can be considered a short term option, because the manufacturing and recycling installations are already available.

Acknowledgements

This project is being partially funded by the European Commission, under the Energy, Environment and Sustainable Development Programme, ENERGIE Contract No. ENK6-CT-2000-00078. The collaboration of the separator supplier partners (Daramic Inc. and Bernard Dumas, S.A.) is also acknowledged.

References

[1] P. Reasbeck, J.G. Smith, Batteries for Automotive Use, Research Studies Press Ltd., 1997, pp. 117–141.
[2] F. Trinidad, F. Sáez, J. Valenciano, J. Power Sources 95 (2001) 24–37.
[3] ENERGIE Project NNE5-1999-20109, Contract ENK6-CT-2000-00078.
[4] D. Linden, T.B. Reddy (Eds.), Handbook of Batteries, third ed., McGraw-Hill, New York, 2002, pp. 24.43–24.45.
[5] M.L. Soria, J. Valenciano, A. Ojeda, G. Raybaut, K. Ihmels, J. Deiters, N. Clement, J. Morales, L. Sánchez, J. Power Sources 116 (2003) 61–72.
[6] R.F. Nelson, Batteries Int. 43 (2000) 51–60.